Check for updates

Received: 24 July 2020 | Revised: 28 September 2021 | Accepted: 6 October 2021

DOI: 10.1002/rnc.5852

RESEARCH ARTICLE

WILEY

Robust impulsive observer design for infinite-dimensional cell population balance models

Alexander Schaum | **Pascal Jerono** | **Petro Feketa**

Automation and Control Group, Kiel University, Kiel, Germany

Correspondence
Alexander Schaum, Automation and Control Group, Kiel University, Kaiserstr. 2, 24143 Kiel, Germany.
Email: alsc@tf.uni-kiel.de

Funding information
Deutsche Forschungsgemeinschaft, Grant/Award Number: 395461267

Abstract

The observer design problem for a class of cell population balance models, describing the time evolution of the cell mass density distribution function and the substrate concentration in a continuous-stirred tank bioreactor with irregular discrete-time measurements of the cell mass distribution is considered. The model consists of a partial integro-differential equation coupled with an ordinary differential equation. Using the theory of impulsive systems sufficient conditions for the input-to-state-stability (ISS) of the observation error in the state-space $L^1 \times \mathbb{R}_+$ with respect to the measurement uncertainty are derived in terms of the maximum time between successive measurements and the ISS gain. In absence of measurement uncertainty the convergence conditions imply exponential stability of the observation error dynamics. Besides these rigorous conditions, application-oriented tuning guidelines are established. The theoretical results are illustrated with numerical simulations including a comparison with a continuous–discrete extended Kalman filter based on the numerical approximation, showing that a similar accuracy is achieved when using a finite-dimensional approximation of the proposed impulsive observer scheme with a considerably lower computational effort.

KEYWORDS

cell population balance equations, impulsive observer design, input-to-state stability, partial integro-differential equations

1 | INTRODUCTION

The monitoring of particle size distributions during batch or continuous operations of chemical and biological reactors is of importance in several areas of process control.[1-5] Modern particle size measurement devices make it possible to obtain lumped profile information in discrete time instants. Typically such measurement information is subject to uncertainty, coming from lumping, inaccuracies in the measurement technique and device resolution as well as interferences during the measurement. Observer design based on such measurements thus has to account for these uncertainties in particular.

The problem addressed in the present study consists in observer design for a class of cell population balance models for a continuous bioreactor with sampled measurements of the cell size distribution with irregular sampling instants.

Abbreviation: ISS, input-to-state stability

This is an open access article under the terms of the Creative Commons Attribution-NonCommercial-NoDerivs License, which permits use and distribution in any medium, provided the original work is properly cited, the use is non-commercial and no modifications or adaptations are made.
© 2021 The Authors. *International Journal of Robust and Nonlinear Control* published by John Wiley & Sons Ltd.

This is motivated on the one side by the fact that online sensors, if they exist are often based on photometric devices which become biased due to biofouling and also interfere, for example, with gas bubbles that are present in the reactor due to the required aeration. Off-line measurements on the other side are typically obtained by the operation staff and thus can not be ensured to occur at exact prescribed, regular time instances. Even if these measurements can be in some circumstances obtained automatically, using some sophisticated mechanisms, a reduction of the sampling rate to the minimum necessary is always of interest in order to reduce costs.

The consideration of discrete-time measurement based observer design for bioreactors using finite-dimensional mass balance models is a well-known and well-studied problem, even in the case of irregular sampling. In particular, continuous-discrete Kalman filters have been used in References 6-9, continuous-discrete interval observers in References 10-12, a geometric observer based approach in References 13,14, and moving horizon estimation techniques in References 15,16. Impulsive observer design has been proposed in Reference 17 for the case of irregular biomass measurements with measurement uncertainties. Rigorous conditions for the input-to-state stability (ISS)[18] of the observation error with respect to the measurement uncertainty are established and the maximum allowed sampling interval is put in relation with the stationary ISS gain, that is, the uncertainty dependent size of confidence region of the observer. Technically the Lyapunov-based approach used in Reference 17 exploits the ISS Lyapunov function approach developed in References 19-21. It should be mentioned that the Lyapunov-based ISS approach is widely used in general purpose nonlinear systems studies. In particular, there is a variety of extensions of the Lyapunov-based ideas to other more complicated classes of impulsive control systems. In particular, we refer the interested reader to the studies of stochastic time-delay systems with impulses,[22-24] event-triggered control,[25] and switching,[26,27] which provide sufficient conditions for the ISS and pth moment exponential stability in a stochastic setting different to the deterministic and delay-free modeling setup used in the present paper. For partial differential equation models ISS has also shown to provide an efficient means for robust design approaches (see, e.g., Reference 28 and references therein).

It must be highlighted that the above mentioned observer design studies focus on unsegregated models that do not account for the particular cell mass distribution, and only consider lumped, finite-dimensional models. These models are described by ordinary differential equations while segregated ones typically are given by hyperbolic partial integro-differential equations[1,3] and thus correspond to infinite-dimensional models, implying a considerable additional mathematical complexity. In many cases the unsegregated models can be obtained from segregated ones by considering the zeroth and first moment of the distribution (see, e.g., Reference 3). This fact has also been widely exploited for moment and discrepancy-based control and observer design approaches for cell population[9,29] and models of crystallization processes[4,5,30,31] that are structurally similar to cell population balance models. Distributed parameter system models with sampled measurements have recently gained considerable interest, while most approaches consider (linear or semilinear) parabolic equations (see Reference 32 and references therein). Best to our knowledge the observer design problem for the infinite-dimensional cell population balance models using sampled cell-size distribution measurements has not been considered in the literature so far.

Based on these considerations, the main question addressed in the present study is how to establish rigorous criteria on the maximum allowed sampling interval for cell population balance models with sampled cell size distribution measurements in such a way that the observer convergence is robust against bounded measurement uncertainties. This question will be addressed using the qualitative theory of impulsive systems to establish robust convergence conditions in terms of the ISS with respect to the measurement uncertainties.

The subsequent sections are organized as follows. The observation problem is formally stated in Section 2. Section 3 summarizes important preliminaries about the cell count model and ISS of interconnected (impulsive) systems. Section 4 contains the main contribution about the non-local robust convergence of the impulsive cell population balance observer which is summarized in Theorem 2. An application-oriented local corollary is derived in Section 5. A numerical simulation study is presented in Section 6. The final conclusions and an outlook are given in Section 7.

NOTATION

The following notation is used in the sequel. The set of non-negative real numbers is denoted by $\mathbb{R}_+$. $L^1(0,1)$ is the space of real-valued, absolutely integrable functions over the domain $[0,1]$ with norm $\|v\|_{L^1} = \int_0^1 |v(m)|\mathrm{d}m < \infty$ for $v \in L^1(0,1)$. $C^k(X_1, X_2)$ denotes the set of at least k-times continuously differentiable functions from X_1 to X_2 and $\mathcal{B}(X_1, X_2)$ the set of bounded functions from X_1 to X_2. The supremum norm of a function $x \in \mathcal{B}([0,\infty), X)$ is denoted by $\|x\|_{X,\infty} = \sup_{t\geq 0} \|x(t)\|_X$ where $\|x\|_X$ denotes the norm in X.

10991239, 2022, 2, Downloaded from https://onlinelibrary.wiley.com/doi/10.1002/mc.5852 by Karlsruher Institut Fur Technologie, Wiley Online Library on [19/11/2026]. See the Terms and Conditions (https://onlinelibrary.wiley.com/terms-and-conditions) on Wiley Online Library for rules of use; OA articles are governed by the applicable Creative Commons License

2 | PROBLEM STATEMENT

Consider the following class of cell population models[1-3,33]

$$\partial_t n(m,t) = -\partial_m[r(m,s)n(m,t)] - D(t)n(m,t) - \Gamma(m,s)n(m,t) + 2\int_m^1 \Gamma(\mu,s)p(m|\mu)n(\mu,t)\mathrm{d}\mu \tag{1a}$$

$$\dot{s}(t) = D(t)(s_e - s(t)) - \int_0^1 r(m,s)n(m,t)\mathrm{dm} \tag{1b}$$

$$n(1,t) = 0 \tag{1c}$$

$$n(m,0) = n_0(m), \quad s(0) = s_0 \tag{1d}$$

$$y(m,t) = n(m,t) + \epsilon(m,t), \quad t \in \mathbb{T} \tag{1e}$$

with $m \in [0,1]$ being the cell mass, $t \in \mathbb{R}_+$ the time, $n : [0,1] \times \mathbb{R}_+ \to \mathbb{R}_+$ the cell mass distribution with $n(\cdot,t) \in L^1(0,1)$ for all $t \geq 0$, $r \in C^1([0,1] \times \mathbb{R}_+, \mathbb{R}_+)$ the cell growth rate function, $s \in C^1(\mathbb{R}_+, \mathbb{R}_+)$ the substrate concentration with feed concentration $s_e \in \mathbb{R}_+$, $\Gamma : [0,1] \times \mathbb{R}_+ \to \mathbb{R}_+$ the cell division rate, $D : \mathbb{R}_+ \to \mathbb{R}_+$ the dilution rate (i.e., the quotient of feed flow rate and reactor volume), $p : [0,1] \times [0,1] \to \mathbb{R}_+$ the partition probability density function, where $p(m|\mu)$ denotes the probability that by division of a cell of mass μ a cell of mass m is produced, and $y(\cdot,t) \in L^1(0,1)$ the measurement at time $t \geq 0$ of the cell mass distribution $n(\cdot,t)$ with a time-varying bounded error $\epsilon(\cdot,t) \in L^1$ with $\|\epsilon\|_{L^1,\infty} \leq \Delta$. It is assumed that the measurement takes place at irregular sampling instants $t \in \mathbb{T} = \{t_1, t_2, \dots\}$ with $0 \leq t_1 < t_2 < \cdots$ and $\lim_{j\to\infty} t_j = \infty$.

Note that the division probability density function p has the properties

$$\text{(i)} \quad \int_0^\mu p(m|\mu)\mathrm{dm} = 1, \qquad \text{(ii)} \quad \forall \mu \leq m : \quad p(m|\mu) = 0, \tag{2}$$

meaning that (i) the probability that when a cell of mass μ is divided some cell of mass $m \leq \mu$ is born is equal to one, and (ii) by cell division no cells larger than the mother cell can be born.

Furthermore, by mass conservation it holds that the total cell mass does not change when cells divide, meaning that Γ and p are such that

$$\int_0^1 m\Gamma(m,s)n(m,t)\mathrm{dm} = \int_0^1 2m\int_m^1 p(m|\mu)\Gamma(\mu,s)n(\mu,s)\mathrm{d}\mu\mathrm{dm} \tag{3}$$

holds true for all n being solutions of (1).

In the sequel the focus is restricted to the case of a linear dependency of r on the cell mass m as discussed in Reference 3, that is,

$$r(m,s) = m\rho(s), \tag{4}$$

with the specific growth rate $\rho \in C^1(\mathbb{R}_+, \mathbb{R}_+)$, and division rates Γ that are proportional to the cell growth rate so that

$$\Gamma(m,s) = \gamma(m)r(m,s) = \gamma(m)m\rho(s) \tag{5}$$

for some function $\gamma \in L^1(0,1)$.

It should be noted that the model (1) has been widely considered for the description of cell populations,[1-3,33] including experimental validations (e.g., for yeast cultures[1,34] and microalgae[35]).

The existence, uniqueness and positivity of solutions $[n(\cdot,t), s(t)]$ in $L^1 \times \mathbb{R}_+$ for the equation set (1) with (4), (5) is shown in Reference 36. In the following we assume that $\exists n^+ < \infty : n(m,t) \leq n^+ \; \forall\, t \geq 0$, what is satisfied in all physically feasible scenarios.

For the class of cell population balance models (1) an impulsive observer with exponentially convergent estimate $[\hat{n}, \hat{s}]^\intercal \in L^1(0,1) \times \mathbb{R}_+$ into a bounded set of size depending on the maximum measurement uncertainty ϵ will be designed in the next section. The formalization of this convergence property is given by the ISS approach,[18,37] which is recalled in Section 3.2. Note that this problem implies a considerable increase in complexity in comparison to the previous study[17]

10991239, 2022, 2, Downloaded from https://onlinelibrary.wiley.com/doi/10.1002/mc.5852 by Karlsruher Institut Fur Technologie, Wiley Online Library on [19/11/2026]. See the Terms and Conditions (https://onlinelibrary.wiley.com/terms-and-conditions) on Wiley Online Library for rules of use; OA articles are governed by the applicable Creative Commons License

where a finite-dimensional mass-balance biomass-substrate model with state in $\mathbb{R}^2_+$ was considered with irregular sampling of the biomass. While the mathematical framework in the $L^1(0,1)\times\mathbb{R}_+$ space considered is quite different, the Lyapunov-based ISS framework exploited in Reference 17 can be applied in the present context also.

Before discussing the proposed impulsive observer design some preliminary considerations about the behavior of the cell count dynamics and the interconnection of impulsive systems follows.

3 | SOME PRELIMINARY CONSIDERATIONS

In this section some important preliminary facts about the cell mass distribution model (1) and the stability analysis of interconnected impulsive systems are summarized.

3.1 | Cell count dynamics

In this section some important facts about the cell count dynamics associated to the cell population balance model (1) are summarized. First, note that given the positivity of solutions n it holds that

$$\|n\|_{L^1} = \int_0^1 |n|\mathrm{d}m = \int_0^1 n\mathrm{d}m = N, \quad \int_0^1 mn\mathrm{d}m = b, \tag{6}$$

meaning that the associated L^1 norm is identical to the total number N of cells in the reactor, that is, the zeroth moment, and the first moment of n is identical to the total biomass b. The following result will be useful in the sequel.

Lemma 1. *Consider (1) with (2), (4), and (5) with n_0 such that $\int_0^1 n_0(m)\mathrm{d}m \in [0, N_0]$, and let $N = \int_0^1 n\mathrm{d}m$. Then the set $\mathcal{M} = [0, M]\times[0, s_e]$ with $M = N_0 + \gamma^+ s_e$ is positively invariant, that is, for all $[N(0)\ \ s(0)]^\intercal \in \mathcal{M}$ it holds that $[N(t)\ \ s(t)]^\intercal \in \mathcal{M}$ for all $t \geq 0$.*

Proof. Considering $s = 0$ it follows from (1b) that $\dot{s} = Ds_e > 0$ and for $s = s_e$ that $\dot{s} = -\rho(s)\int_0^1 mn\mathrm{d}m \leq 0$. Thus for all $s(0) \in [0, s_e]$ it holds that $s(t) \in [0, s_e]$ for all $t \geq 0$. Further, with (4), (5) the associated dynamics of N are given by

$$\begin{aligned}\dot{N} &= \int_0^1 \partial_t n\mathrm{d}m = \int_0^1 \left[\rho(s)\left(-\partial_m(mn) - \gamma mn + 2\int_m^1 p(m|\mu)\gamma\mu n\mathrm{d}\mu\right) - Dn\right]\mathrm{d}m \\ &= -DN + \rho(s)\left(-mn\Big|_0^1 - \int_0^1\left(\gamma mn - 2\int_m^1 p(m|\mu)\gamma\mu n\mathrm{d}\mu\right)\mathrm{d}m\right).\end{aligned}$$

By Fubinis theorem[38] and property (2) it follows that

$$\int_0^1 2\int_m^1 p(m|\mu)\gamma\mu n\mathrm{d}\mu\mathrm{d}m = 2\int_0^1\int_0^\mu p(m|\mu)\mathrm{d}m\gamma\mu n\mathrm{d}\mu = 2\int_0^1 \gamma\mu n\mathrm{d}\mu = 2\int_0^1 \gamma mn\mathrm{d}m.$$

With this relation and using the boundary condition (1c) it follows that

$$\dot{N} = -DN + \rho(s)\int_0^1 \gamma mn\mathrm{d}m, \quad N(0) = N_0.$$

Given the positivity of the solution n, it holds that $N = 0$ if and only if $n = 0$ and thus $\dot{N} = 0$. By the same positivity property the integral term can be bounded as follows

$$\int_0^1 \gamma mn\mathrm{d}m \leq \gamma^+\int_0^1 mn\mathrm{d}m = \gamma^+ b$$

with the maximum value γ^+ of γ and the total biomass b as defined in (6). Summarizing

$$\dot{N} \leq -DN + \rho(s)\gamma^+ b.$$

10991239, 2022, 2, Downloaded from https://onlinelibrary.wiley.com/doi/10.1002/mc.5852 by Karlsruher Institut Fur Technologie, Wiley Online Library on [19/11/2026]. See the Terms and Conditions (https://onlinelibrary.wiley.com/terms-and-conditions) on Wiley Online Library for rules of use; OA articles are governed by the applicable Creative Commons License

Introducing the variable $w = N + \gamma^+ s$ it follows that

$$\begin{aligned}\dot{w} &= -DN + \rho(s)\int_0^1 \gamma m n \mathrm{dm} + \gamma^+ D(s_e - s) - \gamma^+ \rho(s) b \\ &= -D(w - \gamma^+ s_e) + \rho(s)\left(\int_0^1 \gamma m n \mathrm{dm} - \gamma^+ b\right) \\ &\leq -D(w - \gamma^+ s_e) + \rho(s)\left(\gamma^+ \int_0^1 m n \mathrm{dm} - \gamma^+ \int_0^1 m n \mathrm{dm}\right) \\ &= -D(w - \gamma^+ s_e).\end{aligned}$$

This shows that for $w(0) \leq \gamma^+ s_e$ it holds that $w(t) \leq \gamma^+ s_e$ and for $w(0) \geq \gamma^+ s_e$ it follows that $w(t) \leq w(0)$. In consequence, for $\int_0^1 n_0 \mathrm{dm} \leq N_0$ it holds that $N(t) + \gamma^+ s(t) = w(t) \leq \max\{\gamma^+ s_e, N_0 + \gamma^+ s_0\} \leq N_0 + \gamma^+ s_e$ and thus $N(t) \leq N_0 + \gamma^+ s_e = M$. Consequently for all n_0 so that $\int_0^1 n_0(m) \mathrm{dm} \leq N_0$ it holds that $N(t) \in [0, M]$. This implies the positive invariance of the set $\mathcal{M} = [0, M] \times [0, s_e]$. ∎

3.2 | Interconnected impulsive systems

The following considerations will be used later to prove the stability of the impulsive observer. The results in this subsection follow the developments in Reference 17.

Let $\mathbb{T} = \{t_1, t_2, \dots\}$ be a strictly increasing sequence of impulse times in (t_0, ∞) for some initial time $t_0 \in \mathbb{R}$ with $t_1 < t_2 < \cdots$ and no finite accumulation point, that is, $\lim_{k\to\infty} t_k = \infty$. The latter condition prevents the occurrence of the Zeno phenomenon[39] that is characterized by an infinite number of impulsive jumps in a finite time. Consider a cascade interconnection with impulsive jumps

$$\begin{aligned}\Sigma_1 &: \dot{x}_1 = f_1(x_1, x_2), \quad t \notin \mathbb{T}, \\ \Sigma_2 &: \dot{x}_2 = f_2(x_2), \quad t \in \mathbb{R}, \\ \Sigma_{imp} &: x_1 = g_1(x_1^-, u^-), \quad t \in \mathbb{T},\end{aligned} \tag{7}$$

where $t \in \mathbb{R}$ denotes the time, $x_1(t) \in X_1, x_2(t) \in X_2$ the states with some metric spaces X_1, X_2, $u \in \mathcal{B}([t_0, \infty), \mathcal{U})$ an external input with $\mathcal{U}$ a metric space so that $\|u\|_{\mathcal{U},\infty} := \sup_{t \geq t_0} \|u(t)\|_{\mathcal{U}} < \infty$, where $\|\cdot\|_{\mathcal{U}}$ stands for the norm induced by the metric in $\mathcal{U}$. Further, $f_1 : X_1 \times X_2 \to X_1$ and $f_2 : X_2 \to X_2$ are such that there exist a unique global solution to (7). The state $x = [x_1, x_2]^\intercal$ and the external input u are assumed to be right-continuous and to have left limits at all times. Denote by $(\cdot)^-$ the left-limit operator, that is, $x^-(t) = \lim_{s \uparrow t} x(s)$.

For a given set $\mathbb{T}$, we denote by $\boldsymbol{x} = \boldsymbol{x}(\cdot\,; t_0, \boldsymbol{x}_0, u)$ a piecewise-continuous function from $[t_0, \infty)$ to $X_1 \times X_2$ that is a solution to (7) corresponding to the initial data $(t_0, \boldsymbol{x}_0) \in \mathbb{R} \times X_1 \times X_2$ and input $u \in \mathcal{B}([t_0, \infty), \mathcal{U})$. The existence and uniqueness of such a solution is assumed in the following. The norm of the state $\boldsymbol{x} \in X_1 \times X_2$ is denoted by $\|\boldsymbol{x}\|$.

For the purpose of defining a suitable notion of stability recall the following definitions of comparison functions:[37,40]

- $\alpha \in \mathcal{P}$ if $\alpha : [0, \infty) \to [0, \infty)$ is continuous, $\alpha(0) = 0$, and $\alpha(r) > 0$ for all $r > 0$;
- $\alpha \in \mathcal{P}_L$ if $\alpha \in \mathcal{P}$ and it is globally Lipschitz continuous, that is, $\exists\, L > 0$ such that $|\alpha(s_1) - \alpha(s_2)| \leq L|s_1 - s_2|$ for all $s_1, s_2 \in [0, \infty)$;
- $\alpha \in \mathcal{K}$ if $\alpha \in \mathcal{P}$ and it is strictly increasing;
- $\alpha \in \mathcal{K}_\infty$ if $\alpha \in \mathcal{K}$ and it is unbounded;
- $\beta \in \mathcal{KL}$ if $\beta : [0, \infty) \times [0, \infty) \to [0, \infty)$ is continuous, $\beta(\cdot, t)$ is of class $\mathcal{K}$ for each fixed $t \geq 0$ and for each fixed $r \geq 0$ the function $\beta(r, \cdot)$ is strictly decreasing with $\lim_{t\to\infty} \beta(r, t) = 0$.

Definition 1. For a given sequence $\mathbb{T}$ of impulse times we call system (7) input-to-state stable (ISS) if there exist functions $\beta \in \mathcal{KL}$ and $\zeta \in \mathcal{K}_\infty$ such that for every initial data $(t_0, \boldsymbol{x}_0) \in \mathbb{R} \times X_1 \times X_2$ and every input $u \in \mathcal{B}([t_0, \infty), \mathcal{U})$, the corresponding solution to (7) exists globally and satisfies

$$\|\boldsymbol{x}(t; t_0, x_0, u)\| \leq \beta(\|x_0\|, t - t_0) + \zeta(\|u\|_{\mathcal{U},\infty}) \quad \forall t \geq t_0. \tag{8}$$

10991239, 2022, 2, Downloaded from https://onlinelibrary.wiley.com/doi/10.1002/rnc.5852 by Karlsruher Institut Fur Technologie, Wiley Online Library on [19/11/2026]. See the Terms and Conditions (https://onlinelibrary.wiley.com/terms-and-conditions) on Wiley Online Library for rules of use; OA articles are governed by the applicable Creative Commons License

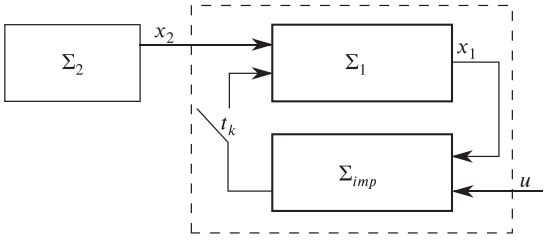


FIGURE 1 Interconnection structure of system (7) with impulses at times $t_k,\ k \in \mathbb{N}$. The dashed box indicates the impulsive system $(\Sigma_1, \Sigma_{\text{imp}})$ with the two inputs x_2 and u

The cascade structure of the interconnection (7) suggests to consider x_2 as an external input to the system Σ_1 with the state x_1 (see Figure 1). By $x_2 = x_2(t; t_0, x_{20})$ we denote a solution to Σ_2 satisfying the initial condition $x_2(t_0) = x_{20}$. In the following it is assumed that the solution remains bounded for all times, that is, $\|x_2\|_{X_2,\infty} = \sup_{t\geq t_0} \|x_2(t)\|_{X_2} < \infty$. For a given initial value $x_{10} \in X_1$ and inputs $x_2 \in \mathcal{B}([t_0, \infty), X_2)$, $u \in \mathcal{B}([t_0, \infty), \mathcal{U})$ denote by $x_1 = x_1(t; t_0, x_{10}, (x_2, u))$ the corresponding solution to (Σ_1, Σ_{imp}). The following definition specifies the ISS property for the given case of a system with two inputs.

Definition 2. For a given sequence $\mathbb{T}$ of impulse times we call system (Σ_1, Σ_{imp}) input-to-state stable (ISS) from (x_2, u) to x_1 if there exist functions $\beta \in \mathcal{KL}$ and $\zeta_a, \zeta_b \in \mathcal{K}_\infty$ such that for every initial data $(t_0, x_{10}) \in \mathbb{R} \times X_1$ and all inputs $x_2 \in \mathcal{B}([t_0, \infty), X_2)$ and $u \in \mathcal{B}([t_0, \infty), \mathcal{U})$, the corresponding solution x_1 to (Σ_1, Σ_{imp}) exists globally with $x_1(t) \in X_1$ for all $t \geq t_0$ and satisfies

$$\|x_1(t; t_0, x_{10}, (x_2, u))\|_{X_1} \leq \beta(\|x_{10}\|_{X_1}, t - t_0) + \max\left\{\zeta_a(\|x_2\|_{X_2,\infty}), \zeta_b(\|u\|_{\mathcal{U},\infty})\right\} \quad \forall t \geq t_0. \tag{9}$$

For a proper characterization of the ISS property of the system (Σ_1, Σ_{imp}) the following concept of a candidate ISS-Lyapunov function is adapted* from References 20,41.

Definition 3.

- For a given solution $x_2 \in \mathcal{B}([t_0, \infty), X_2)$ of Σ_2 the Dini derivative $\dot{V}_D(x_1)$ is defined by

$$\dot{V}_D(x_1) = \lim_{t\to 0+} \frac{V(\phi_c(t; 0, x_1, x_2)) - V(x_1)}{t},$$

  where ϕ_c is a transition map that corresponds to the continuous part of the system Σ_1, that is, $\phi_c(t; t_0, x_1, x_2)$ is the state of the system Σ_1 at time t if the state at time $t_0 := 0$ is equal to x_1 and no impulses have occurred.
- A Lipschitz continuous function $V : X_1 \to [0, \infty)$ is called a candidate ISS-Lyapunov function for system Σ_1 if $\exists \alpha_1, \alpha_2 \in \mathcal{K}_\infty$ such that

$$\alpha_1(\|x_1\|_{X_1}) \leq V(x_1) \leq \alpha_2(\|x_1\|_{X_1}) \quad \forall x_1 \in X_1 \tag{10}$$

  as well as $\zeta_2, \zeta_u, \pi \in \mathcal{K}_\infty$, and rate functions $\varphi \in \mathcal{P}_L$ and $\psi \in \mathcal{P}$ such that for all $x_1 \in X_1, \chi \in X_2, \xi \in \mathcal{U}$

$$\begin{aligned} V(x_1) \geq \max\{\zeta_2(\|\chi\|_{X_2}), \zeta_u(\|\xi\|_{\mathcal{U}})\} &\Rightarrow \begin{cases} \dot{V}_D(x_1) \leq \varphi(V(x_1)), \\ V(g_1(x_1, \xi)) \leq \psi(V(x_1)) \end{cases} \\ V(x_1) \leq \max\{\zeta_2(\|\chi\|_{X_2}), \zeta_u(\|\xi\|_{\mathcal{U}})\} &\Rightarrow V(g_1(x_1, \xi)) \leq \pi(\max\{\zeta_2(\|\chi\|_{X_2}), \zeta_u(\|\xi\|_{\mathcal{U}})\}) \end{aligned} \tag{11}$$

  hold true $\forall\, x_2 \in \mathcal{B}([t_0, \infty), X_2)$ with $x_2(t_0) = \chi$.

Having these concepts at hand the following theorem provides sufficient conditions on the stability of the interconnection (7), extending the result from Reference 17.

*The definition of a candidate ISS-Lyapunov function in References 20,41 allows for both positive and negative values of φ. Here $\varphi \in \mathcal{P}_L$ since the continuous dynamics of Σ_1 is supposed to be unstable in the sequel.

10991239, 2022, 2, Downloaded from https://onlinelibrary.wiley.com/doi/10.1002/rnc.5852 by Karlsruher Institut Fur Technologie, Wiley Online Library on [19/11/2026]. See the Terms and Conditions (https://onlinelibrary.wiley.com/terms-and-conditions) on Wiley Online Library for rules of use; OA articles are governed by the applicable Creative Commons License

Theorem 1. *Let for system (7) the following assumptions hold true*

(A1) system Σ_2 is globally asymptotically stable;
(A2) for the impulsive system (Σ_1, Σ_{imp}) there exists a candidate ISS-Lyapunov function $V_1 : X_1 \to [0, \infty)$ with rate functions $\varphi \in \mathcal{P}_L, \psi \in \mathcal{P}$;
(A3) there exists $\gamma > 0$ such that for any $a > 0$

$$\int_{\psi(a)}^{a} \frac{ds}{\varphi(s)} \geq T + \gamma, \tag{12}$$

where $T = \max_{i\in\mathbb{N}}(t_{i+1} - t_i)$ is the maximum distance between two consecutive impulses.

Then, system (7) is ISS with respect to $u \in \mathcal{B}([t_0, \infty), \mathcal{U})$.

Proof. Conditions (A2), (A3) imply the ISS of (Σ_1, Σ_{imp}) w.r.t to (x_2, u) following the reasoning of References 20,41. The ISS of the entire system interconnection (7) follows from standard cascade arguments. ∎

The concepts presented in this subsection are used for the design of an impulsive observer for the cell population balance model (1) in the next section.

4 | IMPULSIVE CELL MASS DISTRIBUTION OBSERVER

In this section an impulsive observer for estimating the cell mass distribution and substrate concentration according to (1) is designed using the general result of Theorem 1. For this purpose the spaces are identified as $X_1 = L^1(0,1)$, $X_2 = \mathbb{R}$ and $\mathcal{U} = L^1(0,1)$. Accordingly, $x_1 \in C(\mathbb{R}_+, L^1(0,1))$, $x_2 \in C(\mathbb{R}_+, \mathbb{R}_+)$, and $u \in \mathcal{B}(\mathbb{T}, L^1(0,1))$. Following the reasoning for the finite-dimensional setup in Reference 17, first a state transformation is introduced which exploits the existence of a reaction invariant[42,43]

$$\boldsymbol{x}(t) := \begin{bmatrix} n(\cdot,t) \\ s(t) \end{bmatrix} \to \begin{bmatrix} n(\cdot,t) \\ \nu(t) \end{bmatrix}, \quad \nu(t) = \overline{n}(t) + s(t), \quad \overline{n}(t) = \int_0^1 mn(m,t)\mathrm{d}m \tag{13}$$

with the first moment $\overline{n}$ of the distribution n. The dynamics of ν are given by

$$\begin{aligned}
\dot{\nu} &= \int_0^1 m\partial_t n \mathrm{d}m + \dot{s} \\
&= \int_0^1 m\left(-\rho(s)\partial_m(mn) - \rho(s)\gamma mn - Dn + 2\int_m^1 \rho(s)p(m|\mu)\gamma\mu n \mathrm{d}\mu\right)\mathrm{d}m + D(s_e - s) - \rho(s)\int_0^1 mn\mathrm{d}m \\
&= D(s_e - \nu) - \rho(s)\left[\int_0^1 mn\mathrm{d}m + \int_0^1 m\left(\partial_m(mn) + \gamma mn - 2\int_m^1 p(m|\mu)\gamma\mu n\mathrm{d}\mu\right)\mathrm{d}m\right].
\end{aligned}$$

In virtue of (3) the last two terms cancel out. Additionally, it holds that

$$\int_0^1 m\partial_m(mn)\mathrm{d}m = m^2 n\Big|_0^1 - \int_0^1 mn\mathrm{d}m$$

so that the complete bracket becomes zero implying that

$$\dot{\nu} = -D(\nu - s_e), \quad \nu(0) = \nu_0 = \overline{n}(0) + s_0. \tag{14}$$

Next, considering the relations (4) and (5) the impulsive observer is set as

$$\partial_t \hat{n}(m,t) = -\rho(\hat{s})\partial_m[m\hat{n}(m,t)] - D(t)\hat{n}(m,t) - \gamma(m)m\rho(\hat{s})\hat{n}(m,t) + 2\int_m^1 \gamma(\mu)\mu\rho(\hat{s})p(m|\mu)\hat{n}(\mu,t)\mathrm{d}\mu, \quad t \notin \mathbb{T} \tag{15a}$$

10991239, 2022, 2, Downloaded from https://onlinelibrary.wiley.com/doi/10.1002/mc.5852 by Karlsruher Institut Fur Technologie, Wiley Online Library on [19/11/2026]. See the Terms and Conditions (https://onlinelibrary.wiley.com/terms-and-conditions) on Wiley Online Library for rules of use; OA articles are governed by the applicable Creative Commons License

$$\hat{n}(1,t) = 0, \quad \hat{n}(m,0) = \hat{n}_0(m)$$
$$\hat{n}(m,t) = (1 - l(m))\hat{n}^-(m,t) + l(m)y(m,t), \quad t \in \mathbb{T} \tag{15b}$$

$$\dot{\hat{v}}(t) = -D(t)(\hat{v} - s_e(t)), \quad \hat{v}(0) = \hat{v}_0 \quad t \geq 0 \tag{15c}$$

$$\hat{s}(t) = \hat{v}(t) - \hat{\overline{n}}(t), \quad \hat{\overline{n}}(t) = \int_0^1 m\hat{n}(m,t)\mathrm{d}m \tag{15d}$$

with the correction gain $l \in L^1(0,1)$. The following main result states conditions on the convergence of the observer in the sense of its ISS with respect to the measurement uncertainty $\epsilon(\cdot,t) \in L^1(0,1), t \in \mathbb{T}$.

Theorem 2. *Consider the cell population balance model (1) with (2), (4), (5) together with the impulsive observer (15). Let* $\int_0^1 n_0(m)\mathrm{d}m \leq N_0$, $\rho^+ = \max_{s\in[0,s_e]}\rho(s)$, L_ρ *the Lipschitz constant of* ρ, $\overline{\gamma} = \int_0^1 m\gamma(m)\mathrm{d}m$, $\gamma^+ = \max_{m\in[0,1]}\gamma(m)$ *and* $\exists\ \lambda,\omega,\delta > 0$ *so that* $0 \leq \varpi = \int_0^1 |1 - l(m)|\mathrm{d}m < 1 - \lambda$. *Then there exists* $K > 0$ *so that, if the maximum time between measurement samples satisfies*

$$T = \max_{k\in\mathbb{N}}(t_{k+1} - t_k) \leq \frac{\log\left(\frac{1}{\varpi+\lambda}\right)}{\omega + \rho^+\overline{\gamma} + (K + 3\overline{\gamma}(N_0 + \gamma^+ s_e))L_\rho - D} - \delta, \tag{16}$$

the observation error dynamics associated to the impulsive observer is ISS with respect to the bounded measurement uncertainty $\epsilon(\cdot,t) \in L^1(0,1), t \in \mathbb{T}$ *in (1e).*

Proof. Introducing the function

$$\tilde{\rho}(\tilde{s},s) = \rho(s + \tilde{s}) - \rho(s) \tag{17}$$

and the associated cell mass observation error $\tilde{n} = \hat{n} - n$ with

$$\begin{aligned}
\partial_t\tilde{n}(m,t) &= -\rho(\hat{s})\partial_m[m\tilde{n}(m,t)] - \tilde{\rho}(\tilde{s},s)\partial_m[mn(m,t)] - \gamma(m)m\left[\tilde{\rho}(\tilde{s},s)n(m,t) + \rho(\hat{s})\tilde{n}(m,t)\right] \\
&\quad + 2\rho(\hat{s})\int_m^1 \gamma(\mu)\mu p(m|\mu)\tilde{n}(\mu,t)\mathrm{d}\mu + 2\tilde{\rho}(\tilde{s},s)\int_m^1 \gamma(\mu)\mu p(m|\mu)n(\mu,t)\mathrm{d}\mu - D(t)\tilde{n}(m,t), \qquad t \notin \mathbb{T} \\
\tilde{n}(1,t) &= 0, \quad \tilde{n}(m,0) = \tilde{n}_0(m) = \hat{n}_0(m) - n_0(m) \\
\tilde{n}(m,t) &= (1 - l(m))\tilde{n}^-(m,t) + l(m)\epsilon(m,t), \qquad t \in \mathbb{T}
\end{aligned}$$

where $\tilde{s} = \hat{s} - s$ is the substrate observation error. Grouping terms one obtains the observation error dynamics

$$\begin{aligned}
\partial_t\tilde{n}(m,t) &= \rho(\hat{s})\left[-\partial_m[m\tilde{n}(m,t)] - \gamma(m)m\tilde{n} + 2\int_m^1 \gamma(\mu)\mu p(m|\mu)\tilde{n}(\mu,t)\mathrm{d}\mu\right] \\
&\quad + \tilde{\rho}(\tilde{s},s)\left[-\partial_m[mn(m,t)] - \gamma(m)mn + 2\int_m^1 \gamma(\mu)\mu p(m|\mu)n(\mu,t)\mathrm{d}\mu\right] - D(t)\tilde{n}(m,t), \quad t \notin \mathbb{T}
\end{aligned} \tag{18a}$$

$$\begin{aligned}
\tilde{n}(1,t) &= 0, \quad \tilde{n}(m,0) = \tilde{n}_0(m) = \hat{n}_0(m) - n_0(m) \\
\tilde{n}(m,t) &= (1 - l(m))\tilde{n}^-(m,t) + l(m)\epsilon(m,t), \quad t \in \mathbb{T}
\end{aligned} \tag{18b}$$

$$\dot{\tilde{v}}(t) = -D(t)\tilde{v}, \quad \tilde{v}(0) = \tilde{v}_0 = \hat{v}_0 - v_0 \quad t \geq 0 \tag{18c}$$

$$\tilde{s}(t) = \tilde{v}(t) - \int_0^1 m\tilde{n}(m,t)\mathrm{d}m. \tag{18d}$$

Consider the function

$$v(t) = V(\tilde{n}(m,t)) = \int_0^1 |\tilde{n}(m,t)|\mathrm{d}m = \|\tilde{n}\|_{L^1}(t) \tag{19}$$

10991239, 2022, 2, Downloaded from https://onlinelibrary.wiley.com/doi/10.1002/rnc.5852 by Karlsruher Institut Fur Technologie, Wiley Online Library on [19/11/2026]. See the Terms and Conditions (https://onlinelibrary.wiley.com/terms-and-conditions) on Wiley Online Library for rules of use; OA articles are governed by the applicable Creative Commons License

with

$$\begin{aligned}\dot{v} &= \int_0^1 \sigma(\tilde{n})\partial_t \tilde{n}\mathrm{dm} \\ &= -Dv + \rho(\hat{s})\int_0^1 \sigma(\tilde{n})\left(-\partial_m(m\tilde{n}) - \gamma m\tilde{n} + 2\int_m^1 p(m|\mu)\gamma\mu\tilde{n}\mathrm{d}\mu\right)\mathrm{dm} \\ &\quad + \tilde{\rho}(\tilde{s}, s)\int_0^1 \sigma(\tilde{n})\left(-\partial_m(mn) - \gamma mn + 2\int_m^1 p(m|\mu)\gamma\mu n\mathrm{d}\mu\right)\mathrm{dm}\end{aligned}$$

with the sign function $\sigma(\cdot)$. It holds that

$$\begin{aligned}\int_0^1 -\sigma(\tilde{n})\partial_m(m\tilde{n})\mathrm{dm} &= \int_0^1 -\partial_m(m|\tilde{n}|)\mathrm{dm} = -m|\tilde{n}|\Big|_0^1 = 0 \\ \int_0^1 -\sigma(\tilde{n})\partial_m(mn)\mathrm{dm} &= -\sigma(\tilde{n})mn\Big|_0^1 + \int_0^1 \sigma'(\tilde{n})mn\mathrm{dm} \\ &= \int_0^1 \sum_{i\in I(\tilde{n})} a_i(\tilde{n})\delta(m-m_i)mn\mathrm{dm} \\ &= \sum_{i\in I(\tilde{n})} a_i(\tilde{n})m_i n(m_i,t) \\ &\le \sum_{i\in I(\tilde{n})} m_i n(m_i,t) \le N\end{aligned}$$

with $a_i \in \{-1, 1\}$ depending on whether the change in $\sigma(\tilde{n})$ is from positive to negative or vice versa, and some $K > 0$. Further

$$\begin{aligned}&\int_0^1 -\gamma(m)m\sigma(\tilde{n})\tilde{n} + 2\sigma(\tilde{n})\int_m^1 p(m|\mu)\gamma\mu\tilde{n}\mathrm{d}\mu\mathrm{dm} \\ &\overset{Fubini}{=} -\int_0^1 \gamma m|\tilde{n}|\mathrm{dm} + 2\int_0^1\int_0^\mu \sigma(\tilde{n})p(m|\mu)\mathrm{dm}\gamma\mu\tilde{n}\mathrm{d}\mu \\ &= -\int_0^1 \gamma m|\tilde{n}|\mathrm{dm} + 2\int_0^1\int_0^m \sigma(\tilde{n})p(\mu|m)\mathrm{d}\mu\gamma m\tilde{n}\mathrm{dm} \\ &= \int_0^1 \gamma m\left(-|\tilde{n}| + 2\tilde{n}\int_0^m \sigma(\tilde{n})p(\mu|m)\mathrm{d}\mu\right)\mathrm{dm} \\ &\le \int_0^1 \gamma m\left(-|\tilde{n}| + 2|\tilde{n}|\int_0^m p(\mu|m)\mathrm{d}\mu\right)\mathrm{dm} \\ &= \int_0^1 \gamma m\left(-|\tilde{n}| + 2|\tilde{n}|\right)\mathrm{dm} \le \int_0^1 \gamma m\mathrm{dm}\int_0^1 |\tilde{n}|\mathrm{dm} = \overline{\gamma}v\end{aligned}$$

where (2) has been used and $\overline{\gamma}$ is the mean value of γ. For the remaining terms which depend on n it follows that

$$\begin{aligned}&\int_0^1 \sigma(\tilde{n})\left(-\gamma mn + 2\int_m^1 p(m|\mu)\gamma\mu n\mathrm{d}\mu\right)\mathrm{dm} \\ &\overset{Fubini}{=} -\int_0^1 \gamma m\sigma(\tilde{n})n\mathrm{dm} + 2\int_0^1\int_0^\mu \sigma(\tilde{n})p(m|\mu)\mathrm{dm}\gamma\mu n\mathrm{d}\mu \\ &= -\int_0^1 \gamma m\sigma(\tilde{n})n\mathrm{dm} + 2\int_0^1\int_0^m \sigma(\tilde{n})p(\mu|m)\mathrm{d}\mu\gamma mn\mathrm{dm} \\ &= -\int_0^1 \gamma mn\left(\sigma(\tilde{n}) - 2\int_0^m \sigma(\tilde{n})p(\mu|m)\mathrm{d}\mu\right)\mathrm{dm}\end{aligned}$$

10991239, 2022, 2, Downloaded from https://onlinelibrary.wiley.com/doi/10.1002/mc.5852 by Karlsruher Institut Fur Technologie, Wiley Online Library on [19/11/2026]. See the Terms and Conditions (https://onlinelibrary.wiley.com/terms-and-conditions) on Wiley Online Library for rules of use; OA articles are governed by the applicable Creative Commons License

$$
\begin{aligned}
&= \int_0^1 \gamma m n\,(2-\sigma(\tilde{n}))\,\mathrm{dm} \le 3\int_0^1 \gamma m \mathrm{dm} \int_0^1 n \mathrm{dm} \\
&= 3\overline{\gamma}\int_0^1 n \mathrm{dm} \le 3\overline{\gamma} M,
\end{aligned}
$$

with the bound M from Lemma 1. In summary one obtains

$$
\begin{aligned}
\dot{v} &\le (\rho(\hat{s})\overline{\gamma} - D)v + (K + 3\overline{\gamma}M)|\tilde{\rho}(\tilde{s}, s)| \\
&\le (\rho^+\overline{\gamma} - D)v + (K + 3\overline{\gamma}M)L_\rho|\tilde{s}| \\
&= (\rho^+\overline{\gamma} - D)v + (K + 3\overline{\gamma}M)L_\rho \left|\tilde{v} - \int_0^1 m\tilde{n}\mathrm{dm}\right| \\
&\le (\rho^+\overline{\gamma} - D)v + (K + 3\overline{\gamma}M)L_\rho \left(|\tilde{v}| + \int_0^1 m|\tilde{n}|\mathrm{dm}\right) \\
&\le (\rho^+\overline{\gamma} - D)v + (K + 3\overline{\gamma}M)L_\rho\,(|\tilde{v}| + v) \\
&= (\rho^+\overline{\gamma} + (K + 3\overline{\gamma}M)L_\rho - D)v + (K + 3\overline{\gamma}M)L_\rho|\tilde{v}|
\end{aligned}
$$

which holds for $t \notin \mathbb{T}$. As a consequence it holds that

$$
\dot{v} \le -\omega v + (\omega + \rho^+\overline{\gamma} + (K + 3\overline{\gamma}M)L_\rho - D)v + (K + 3\overline{\gamma}M)L_\rho|\tilde{v}|.
$$

Accordingly, for all $\tilde{n}$ so that

$$
V(\tilde{n}) \ge \frac{(K + 3\overline{\gamma}M)L_\rho|\tilde{v}|}{\omega} =: \zeta_v(|\tilde{v}|) \tag{20a}
$$

it follows that

$$
\dot{v} \le (\omega + \rho^+\overline{\gamma} + (K + 3\overline{\gamma}M)L_\rho - D)v =: \varphi(v) \tag{20b}
$$

For $t \in \mathbb{T}$ it follows that

$$
\begin{aligned}
v(t) &= \int_0^1 |(1 - l(m))\tilde{n}^-(m,t) + l(m)\epsilon^-(m,t)|\mathrm{dm} \\
&\le \varpi v^-(t) + \|l\|_{L^1}\|\epsilon^-\|_{L^1}, \quad \varpi = \int_0^1 |(1 - l(m)|\mathrm{dm}
\end{aligned}
$$

so that

$$
v(t) \le (\varpi + \lambda)v^-(t) - \lambda v^-(t) + \|l\|_{L^1}\|\epsilon\|_{L^1}.
$$

In consequence, for all $\tilde{n}$ so that

$$
V(\tilde{n}) \ge \frac{\|l\|_{L^1}\|\epsilon\|_{L^1}}{\lambda} =: \zeta_\epsilon\left(\|\epsilon\|_{L^1}\right) \tag{21a}
$$

one has

$$
v(t) \le (\varpi + \lambda)v^-(t) =: \psi(v^-(t)) \tag{21b}
$$

Thus, the following holds true

$$
V(\tilde{n}) \ge \max\left\{\zeta_\epsilon\left(\|\epsilon\|_{L^1}\right), \zeta_v(|\tilde{v}|)\right\} \Rightarrow \begin{cases} \frac{d}{dt}V(\tilde{n}) \le \varphi(v) & t \notin \mathbb{T} \\ V(\tilde{n}) \le \psi\left(V(\tilde{n}^-)\right), & t \in \mathbb{T} \end{cases}. \tag{22}
$$

10991239, 2022, 2, Downloaded from https://onlinelibrary.wiley.com/doi/10.1002/mc.5852 by Karlsruher Institut Fur Technologie, Wiley Online Library on [19/11/2026]. See the Terms and Conditions (https://onlinelibrary.wiley.com/terms-and-conditions) on Wiley Online Library for rules of use; OA articles are governed by the applicable Creative Commons License

For $t \in \mathbb{T}$ when $V(\tilde{n}) \leq \max\{\zeta_\epsilon(\|\epsilon\|_{L^1}), \zeta_v(|\tilde{v}|)\}$ it follows that

$$\begin{aligned}
v(t) &= \int_0^1 |(1-l(m))\tilde{n}^-(m,t) + l(m)\epsilon^-(m,t)|\mathrm{d}m \\
&\leq \varpi v^-(t) + \|l\|_{L^1}\|\epsilon^-\|_{L^1}, \quad \varpi = \int_0^1 |(1-l(m)|\mathrm{d}m < 1 \\
&\leq \varpi \max\{\zeta_\epsilon(\|\epsilon^-\|_{L^1}), \zeta_v(|\tilde{v}|)\} + \|l\|_{L^1}\|\epsilon^-\|_{L^1} \\
&\leq \varpi \max\{\zeta_\epsilon(\|\epsilon^-\|_{L^1}), \zeta_v(|\tilde{v}|)\} + \|l\|_{L^1}\zeta_\epsilon^{-1}(\max\{\zeta_\epsilon(\|\epsilon^-\|_{L^1}), \zeta_v(|\tilde{v}|)\}) \\
&\leq \underbrace{(\varpi\,\mathtt{id} + \|l\|_{L^1}\zeta_\epsilon^{-1})}_{\in\mathcal{K}_\infty}(\max\{\zeta_\epsilon(\|\epsilon^-\|_{L^1}), \zeta_v(|\tilde{v}|)\}) =: \pi(\max\{\zeta_\epsilon(\|\epsilon^-\|_{L^1}), \zeta_v(|\tilde{v}|)\}),
\end{aligned}$$

where $\mathtt{id}$ denotes the identity map, showing that $V(\tilde{n}) = \|\tilde{n}\|_{L^1}$ is a candidate ISS Lyapunov function for the dynamics (18a) and (18b) according to Definition 3.

Given that $\tilde{v}$ is exponentially stable, the ISS of the observation error with respect to $\epsilon \in L^1(0,1)$ follows from Theorem 1 if the condition

$$\int_{\psi(a)}^{a} \frac{\mathrm{d}s}{\varphi(s)} \geq T + \delta$$

holds true for some $\delta > 0$. With the particular rates φ and ψ defined above in (20b) and (21b), respectively, this condition is identical to

$$T + \delta \leq \frac{1}{\omega + \rho^+\overline{\gamma} + (K + 3\overline{\gamma}M)L_\rho - D}\log\left(\frac{1}{\varpi + \lambda}\right)$$

or equivalently (16). ∎

Remark 1. The preceding existence-type result establishes rigorous conditions for ISS of the combined cell-mass distribution and substrate concentration error with respect to the norm $\|\tilde{\boldsymbol{x}}\| = \|\tilde{n}\|_{L^1} + |\tilde{s}|$. Most results in the literature on stability of particulate processes in general (see, e.g., References 4,5,9,29-31,44 and references therein) focus on stability with respect to moments of the distribution. Given that stability in the L^1 norm implies stability of any moment, the present result is much stronger in nature.

Remark 2. The main degrees of freedom in the observer are the correction gain function $l : [0,1] \to \mathbb{R}$ and the constants $\omega, \lambda > 0$. Their interplay is summarized in inequality (16). The main requirement is that the maximum sampling time T is positive. Actually, the choice of the degrees of freedom could be carried out following an optimization procedure maximizing T.

Remark 3. The bound derived in Theorem 2 is rather conservative, given that typically the cell division rate γ takes large values for large m while the associated cell size distribution has a maximum for small values of m. In consequence, the bound for $\int_0^1 m\gamma n\mathrm{d}m$ used in the proof of the theorem is typically too rough. In practical situations the norm will present a much lower gain then in the presented worst case scenario, which nevertheless is necessary to obtain a global estimate. In consequence, for practical applications a local bound which can be handled within a tuning procedure is preferrable.

5 | A LOCAL, APPLICATION ORIENTED RESULT

As pointed out in Remark 3 the global bound derived in Theorem 2 is unnecessarily conservative for practical situations as the maximum bounds are expected to be scarcely observed in a real process. Thus a local result is probably more suited for implementation in a real scenario. For this purpose recall that $\|\epsilon\|_{L^{1,\infty}} \leq \Delta$ and assume that the growth rate of the continuous evolution of the Lyapunov function $V(\tilde{n})$ defined in (19) can be locally approximated by

$$\dot{v} \leq \kappa v, \qquad t \notin \mathbb{T}, \quad v \geq \chi_1|\tilde{s}| \tag{23a}$$

$$v \leq (\lambda + \varpi)v^-, \qquad t \in \mathbb{T}, \quad v \geq \frac{1-\varpi}{\lambda}\Delta \tag{23b}$$

$$v \leq \left(\varpi + (1-\varpi)\frac{\lambda}{1-\varpi}\right)v^- = (\lambda + \varpi)v^-, \qquad t \in \mathbb{T}, \quad v \leq \frac{1-\varpi}{\lambda}\Delta \tag{23c}$$

10991239, 2022, 2, Downloaded from https://onlinelibrary.wiley.com/doi/10.1002/mc.5852 by Karlsruher Institut Fur Technologie, Wiley Online Library on [19/11/2026]. See the Terms and Conditions (https://onlinelibrary.wiley.com/terms-and-conditions) on Wiley Online Library for rules of use; OA articles are governed by the applicable Creative Commons License

for some constant $\kappa, \chi_1 > 0$, given that the gain ζ_ϵ is linear. In (23) κ is a local tuning parameter, and ϖ depends on the correction gain function l. Note that for a constant correction gain $l(m) = l$ for all $m \in [0, 1]$ it holds that $\varpi = 1 - l$ and (23b) coincides with (21b). Actually, the rate κ can be estimated, for example, using simulation results or experimental data. For this slightly modified setup the following corollary is obtained.

Corollary 1. *Let the assumptions of Theorem 2 and additionally (23) hold true for some $\kappa, \chi_1, \lambda > 0$ and let $l = const. > 0$, so that $\varpi = 1 - l$ and $\|l\|_{L^1} = l$. Then the estimation error dynamics (18) $\tilde{\boldsymbol{x}}$ is ISS with respect to the measurement uncertainty $\epsilon \in L^1$ with $0 < \|\epsilon\|_{L^1} \leq \Delta$ if*

$$T = \max_{k\in\mathbb{N}}(t_{k+1} - t_k) \leq \frac{1}{\kappa} \ln\left(\frac{1}{\varpi + \lambda}\right) - \delta. \tag{24a}$$

Furthermore, the estimation error converges in finite time into the region defined by the ISS gain

$$\chi(\Delta) = e^{-\kappa\delta} \frac{l}{\lambda} \frac{\Delta}{\lambda + \varpi}. \tag{24b}$$

Proof. With (24a) it follows that

$$\int_{(\lambda+\varpi)a}^{a} \frac{\mathrm{d}s}{s} \geq \kappa(T + \delta),$$

with $T = \max_{k\in\mathbb{N}}(t_{k+1} - t_k)$ so that condition (12) along with Assumptions 1 and 2 of Theorem 1 are satisfied. This implies the ISS of the estimation error with respect to bounded measurement uncertainties ϵ.

To derive the ISS gain χ given in (24b) consider that for some $k \in \mathbb{N}$ it holds that $v(t_k) = \frac{1-\varpi}{\lambda}\Delta$, so that the condition for (23b) is satisfied. Let $t_{k_1} \geq t_*$ with

$$|\tilde{v}(t)| = |\tilde{v}(0)|e^{-\int_0^{t_{k_1}} D(\tau)\mathrm{d}\tau} \leq |\tilde{v}(0)|e^{-\int_0^{t_*} D(\tau)\mathrm{d}\tau} = \frac{1-\varpi}{\lambda}\Delta \tag{25}$$

so that the condition for (23a) is also satisfied. Then it follows from (23a) that for $t \in [t_k, t_{k+1})$

$$v(t) = v(t_k)e^{\kappa t} = \frac{1-\varpi}{\lambda}\Delta e^{\kappa t} \leq \frac{1-\varpi}{\lambda}\Delta e^{\kappa T} \leq \frac{1-\varpi}{\lambda}\frac{\Delta}{\varpi+\lambda}e^{-\kappa\delta} = \chi(\Delta)$$

where (24a) and $1 - \varpi = l$ have been used. Accordingly, if it is ensured that for some finite time t_k it holds that $v(t_k) \leq \frac{1-\varpi}{\lambda}\Delta$ and $t_k \geq t_{k_1}$ with t_{k_1} so that (25) holds true, then the solution of $v = \|\tilde{n}\|_{L^1}$ will be bounded by χ for all $t \geq t_k$. Considering $v(0) \geq \frac{1-\varpi}{\lambda}\Delta$ it follows from (24a) that the sequence $v(t_k)$ is strictly decaying according to

$$v(t_k) \leq v(0)\left(e^{-\kappa\delta}\right)^k$$

so that the required t_k is determined by

$$k \geq k_2 = \log_{e^{-\kappa\delta}}\left(\frac{1-\varpi}{\lambda v(0)}\Delta\right) = -\frac{\ln\left(\frac{1-\varpi}{\lambda v(0)}\Delta\right)}{\kappa\delta}.$$

Accordingly, the above requirements are fulfilled and the solutions $\tilde{n}$ are bounded by χ after a finite time given by $\max\{t_{k_1}, t_{k_2}\}$. ∎

Remark 4. The result stated in Corollary 1 ensures the ISS of the estimation error $\tilde{\boldsymbol{x}}$ locally and thus allows to be considerably less restrictive than the global result of Theorem 2 (see Remark 3). To the authors knowledge this is the first time such a strong result has been shown, ensuring the ISS of the observation error in the $L^1 \times \mathbb{R}_+$ state space. From a theoretical point of view this is thus a great advance in comparison to the convergence results for the moments of the distribution, as they are typically considered in other studies (see, e.g., References 4,5,9,29-31,44). On the other hand, from a practical point of view the question remains open to what extent this approach yields an advantage. This question is addressed in the subsequent section by a comparison with a state of the art estimation technique frequently

10991239, 2022, 2, Downloaded from https://onlinelibrary.wiley.com/doi/10.1002/rnc.5852 by Karlsruher Institut Fur Technologie, Wiley Online Library on [19/11/2026]. See the Terms and Conditions (https://onlinelibrary.wiley.com/terms-and-conditions) on Wiley Online Library for rules of use; OA articles are governed by the applicable Creative Commons License

employed in the process control community, namely the continuous–discrete extended Kalman filter (EKF) (see, e.g., References 9,31,45).

6 | NUMERICAL EXAMPLE

In order to illustrate the theoretical result of Theorem 2 a case example with non-monotonic Haldane growth rate

$$\rho(s) = \frac{k_0 s}{k_s + s + \frac{s^2}{k_i}}, \quad k_0 = 0.2, \quad k_i = 0.2, \quad k_s = 0.3$$

has been considered with $s_e = 1\,\mathrm{g/l}$ and $D = 0.035\,\mathrm{h}^{-1}$. Note that according to the analysis in References 46,47 the mass-balance of the reactor with a continuous measurement of the biomass, that is, the first moment of the distribution, is not observable. Accordingly, the consideration of this case example with an irregular discrete-time measurement of the cell size distribution represents a challenging problem, in particular for the estimation of the substrate concentration s.

In order to prevent problems for transient negative substrate estimates $\rho(s) = 0$ for $s \leq 0$ is set artificially, motivated by the reasoning in Reference 48.

The cell division rate γ and the probability function p are considered as

$$\gamma(m) = \frac{\gamma^+}{2}\left(1.0 + \tanh(\alpha(m - m_0))\right), \quad \gamma^+ = 20, \quad \alpha = 10, \quad m_0 = 0.5$$
$$p(m|\mu) = \frac{1}{B(q)}\frac{1}{\mu}\left(\frac{m}{\mu}\right)^{q-1}\left(1 - \frac{m}{\mu}\right)^{q-1}, \quad B(q) = \frac{f_\gamma(q)^2}{f_\gamma(2q)}, \quad q = 2$$

where p is a symmetric beta distribution[3] and f_γ is the Gamma-function (i.e., the extension of the factorial to the real numbers).

As known from studies on the corresponding mass-balance based biomass and substrate concentration models[49] with a non-monotonic Haldane growth rate function the reactor model can exhibit bistability. Accordingly, the above parameters where chosen so that the reactor has the washout steady-state $[b\ s]^\intercal = [0, s_e]^\intercal$ and a high-conversion steady-state $[\bar{b}\ \bar{s}]^\intercal$ as attractors, where $b = \int_0^1 mn\mathrm{d}m$ is the total biomass in the reactor.

For the numerical solution in MATLAB the space has been discretized using an equally spaced mesh of 60 collocation points and approximating the spatial derivative by means of backward differences and the integral term by means of the trapezoidal rule. The resulting set of odes has been solved using the Runge–Kutta based solver `ode45`. The associated time evolution of the cell mass distribution for initial conditions $\boldsymbol{x}_0, \hat{\boldsymbol{x}}_0$ chosen as

$$\boldsymbol{x}_0 = [n_0, s_0]^\intercal, \quad n_0(z) = 12.14e^{-(z_0.1)^2/0.05^2}, \quad s_0 = 0.8$$
$$\hat{\boldsymbol{x}}_0 = [\hat{n}_0, \hat{s}_0]^\intercal, \quad \hat{n}_0(z) = 6.35e^{-(z_0.4)^2/0.05^2}, \quad \hat{s}_0 = 0.4$$

and lying in opposite domains of attraction is shown in Figure 2 and the associated substrate and biomass concentrations in Figure 3. It can be seen that the state $\boldsymbol{x}$ (left side in Figure 2 and blue continuous curves in Figure 3) slowly converge to the washout state, while $\hat{\boldsymbol{x}}$ (right side in Figure 2 and orange dashed curves in Figure 3) reaches the high conversion equilibrium state after about 150 to 200 time units.

The proposed observer has been set with $l = 0.99 =$cst., and the continuous Lyapunov gain $\varphi(v) = \kappa v$ adapted according to the considerations in Section 5 yielding $\kappa = 0.01$. Considering $\delta = 0.5$, $\lambda = 0.8$ the allowed samples time interval is limited by $\max_{k\in\mathbb{N}}(t_{k+1} - t_k) \approx 20.57$. The minimum time between samples has been set to $\min_{k\in\mathbb{N}}(t_{k+1} - t_k) \approx 10.26$. Considering measurement uncertainty with a maximum offset of $\Delta = 0.1$ the associated ISS gain is determined as $\chi(\Delta) \approx 0.15$.

The measurement uncertainty has been emulated in simulations by a uniform distribution over $[0, 1]$ with minimum and maximum values $\epsilon_{\min} = -\Delta, \epsilon_{\max} = \Delta$.

In order to compare the proposed observer scheme with a state-of-the art technique in process control applications the following simulations additionally include results obtained with an continuous–discrete EKF[9,31,45] based on the finite-dimensional model approximation with data assimilation in the cell mass distribution only, that is, considering the same structure as in (15), but with the correction gain l determined using the approximated observation error covariance

10991239, 2022, 2, Downloaded from https://onlinelibrary.wiley.com/doi/10.1002/rnc.5852 by Karlsruher Institut Fur Technologie, Wiley Online Library on [19/11/2026]. See the Terms and Conditions (https://onlinelibrary.wiley.com/terms-and-conditions) on Wiley Online Library for rules of use; OA articles are governed by the applicable Creative Commons License

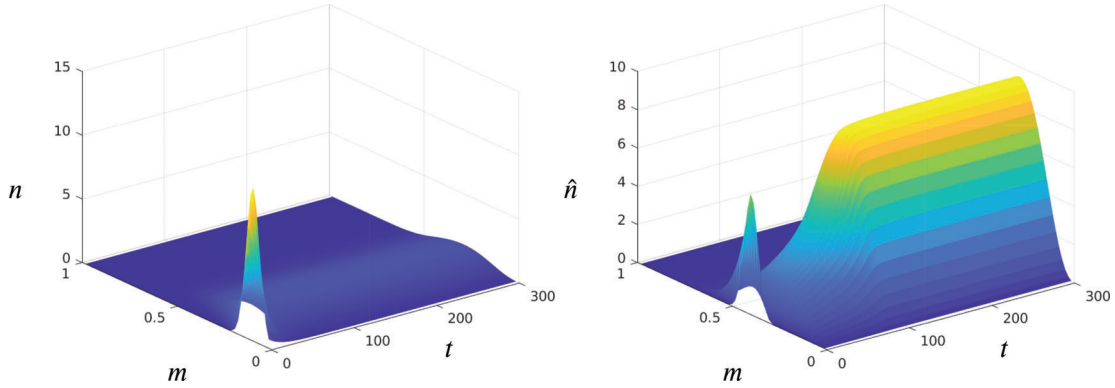


FIGURE 2 Evolution of the cell mass distributions for initial conditions in opposite domains of attraction and without measurement injection

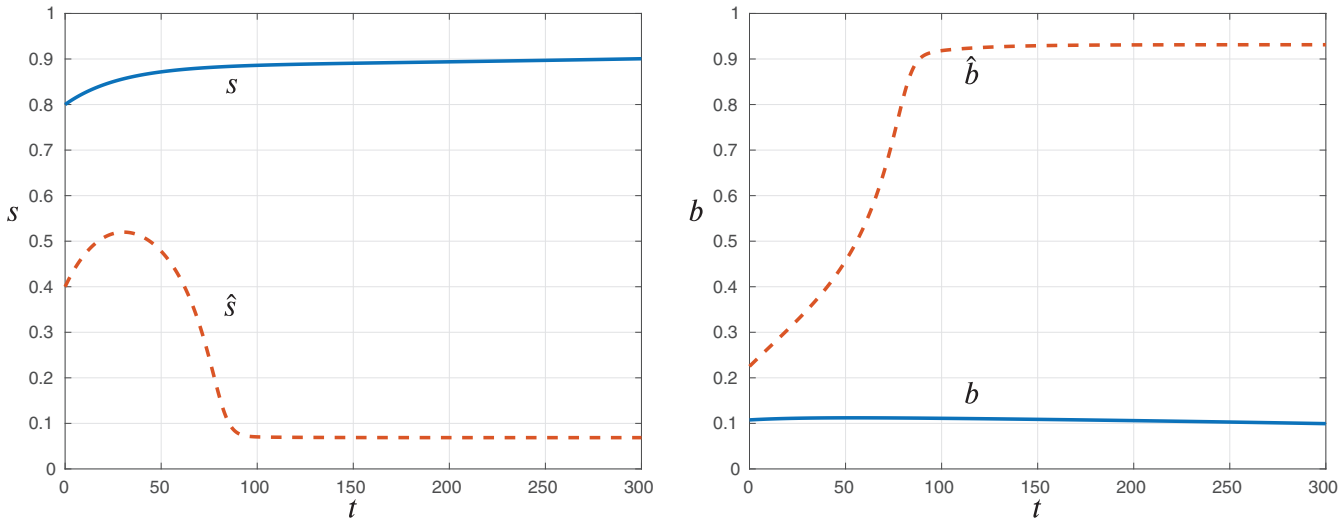


FIGURE 3 Evolution of substrate and biomass concentrations for initial conditions in opposite domains of attraction and without measurement injection

matrix. Note that the calculation of the covariance matrix is based on the associated Ricatti-differential-equation and thus implies a considerable higher computational effort for the EKF in comparison to the proposed scheme.

The resulting time evolution of the cell size distribution and its estimates are shown in Figure 4 and the corresponding substrate and biomass concentrations together with their estimates in Figure 5. The yellow continuous curves correspond to the proposed impulsive observer scheme and the red dashed curves to the EKF. The time evolution of the approximate error norms $\|\tilde{\boldsymbol{x}}\|$ are shown in Figure 6. It can be seen that both estimation schemes yield almost identical results and obtain reliable estimates for the biomass and the cell mass distribution after the second sampling instant. It can be further seen that the observed substrate concentrations converge within approximately 20 time units.

In comparison with the approximated EKF solution the proposed scheme (i) achieves a similar accuracy in its approximated implementation, (ii) has an ensured convergence in the $L^1 \times \mathbb{R}_+$ state-space according to Theorem 2, and (iii) its approximate implementation does not require the solution of the 60×60 matrix Ricatti-differential-equation for the approximate observation error covariance matrix.

Finally, to illustrate the exponential convergence feature in absence of measurement uncertainty, Figure 7 shows the time evolution of the approximate error norm $\|\tilde{\boldsymbol{x}}\|$ for $\Delta = 0$. The simulation validates the exponential convergence in about 120 time units for both schemes.

Remark 5. As commented above, the computational load of the proposed observer scheme is considerably lower than the one of the EKF, given that the covariance matrix does not need to be determined and the observer gains are *a priori*

10991239, 2022, 2, Downloaded from https://onlinelibrary.wiley.com/doi/10.1002/mc.5852 by Karlsruher Institut Fur Technologie, Wiley Online Library on [19/11/2026]. See the Terms and Conditions (https://onlinelibrary.wiley.com/terms-and-conditions) on Wiley Online Library for rules of use; OA articles are governed by the applicable Creative Commons License

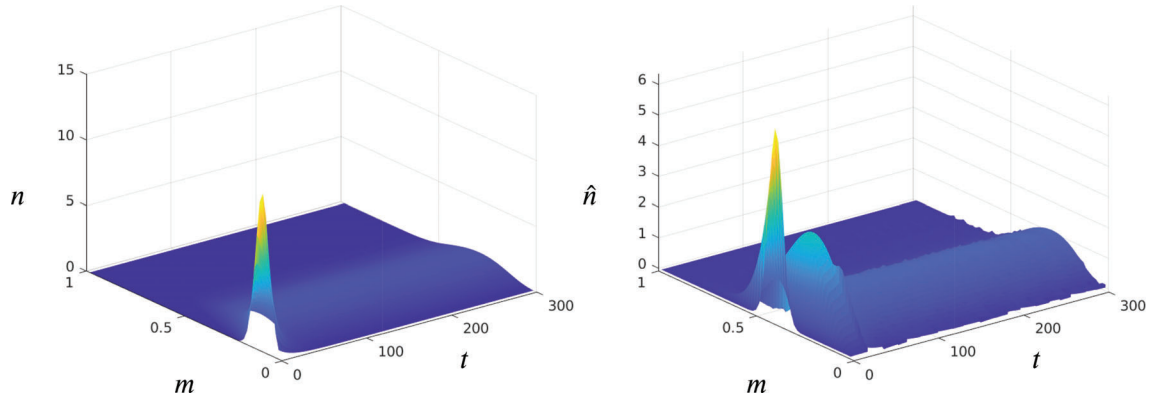


FIGURE 4 Actual cell mass distribution (left) and its estimate (right)

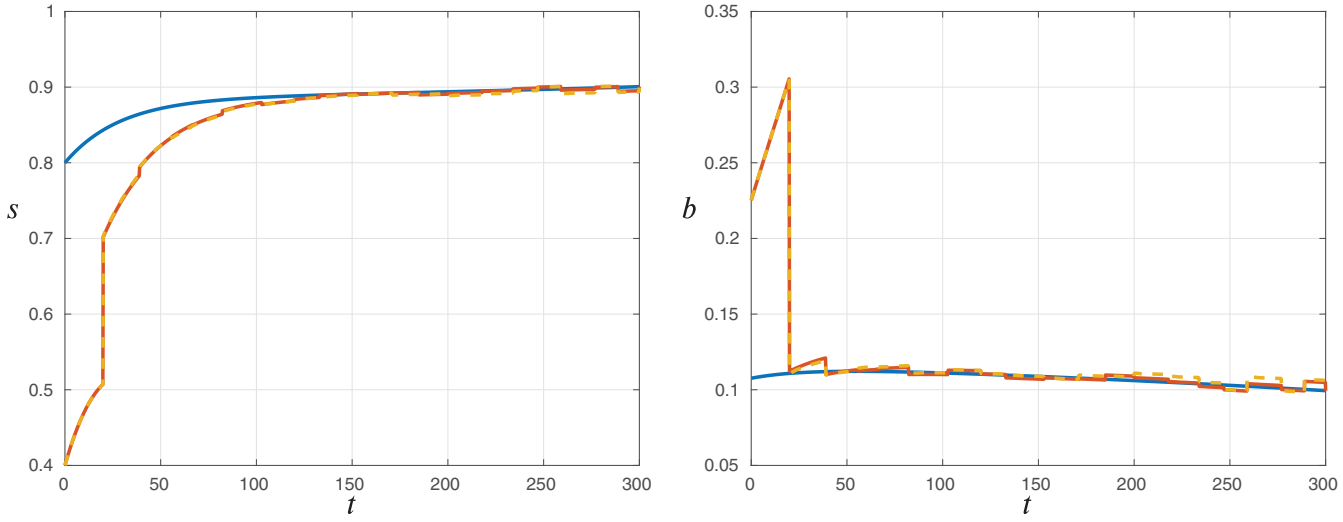


FIGURE 5 Actual (continuous—blue), estimated by Kalman-filter (continuous—red) and estimated by impulsive observer (dashed—yellow) substrate (left) and biomass (right) concentrations

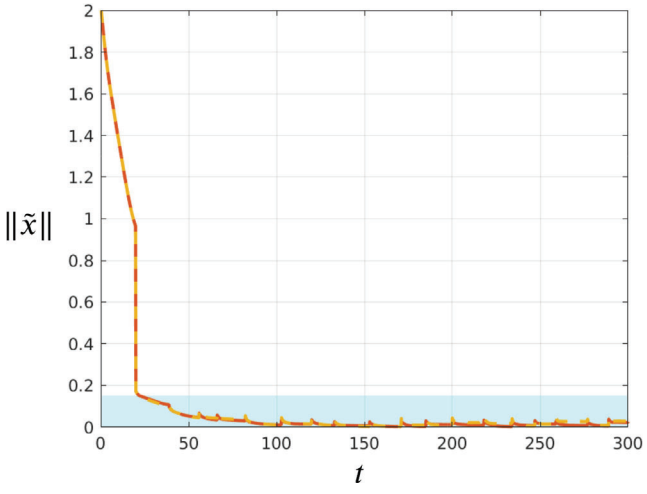


FIGURE 6 Estimation error norm $\|\tilde{x}\|$ of Kalman-filter (continuous—red) and impulsive observer (dashed—yellow) over time. The cyan region corresponds to the predicted ISS gain

10991239, 2022, 2, Downloaded from https://onlinelibrary.wiley.com/doi/10.1002/rnc.5852 by Karlsruher Institut Fur Technologie, Wiley Online Library on [19/11/2026]. See the Terms and Conditions (https://onlinelibrary.wiley.com/terms-and-conditions) on Wiley Online Library for rules of use; OA articles are governed by the applicable Creative Commons License

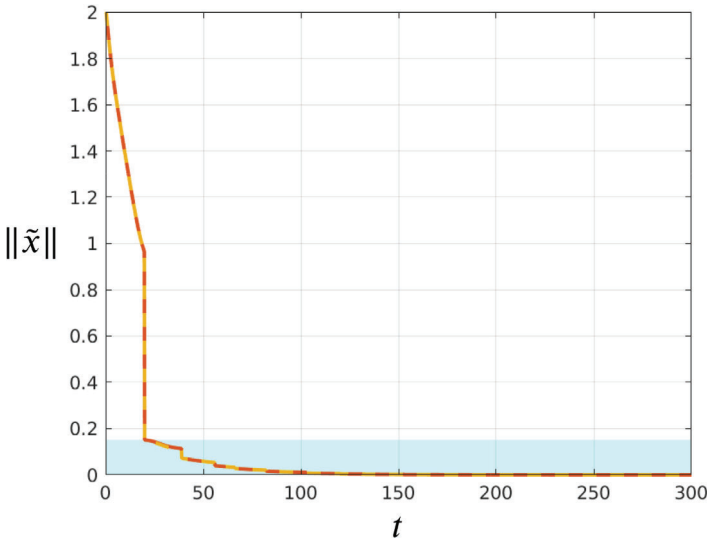


FIGURE 7 Estimation error norm $\|\tilde{x}\|$ of Kalman-filter (continuous—red) and impulsive observer (dashed—yellow) over time in absence of measurement uncertainty

calculated on the basis of Theorem 2 or Corollary 1. On the other side, the computational effort associated to obtain a good approximation of the solution of the partial integro–differential Equation (1) is the same for both state estimation schemes. This computational effort can be optimized for practical purposes following, for example, the steps outlined in References 50,51 trying to achieve a good compromise between numerical accuracy, practical relevant perturbations and sensor uncertainty level.

7 | CONCLUSIONS AND OUTLOOK

7.1 | Conclusions

An impulsive observer is designed for the estimation of the continuous time evolution of the cell mass density distribution and substrate concentration in a stirred tank bioreactor with irregularly sampled measurements of the cell mass distribution. A sufficient condition for the ISS of the estimation error in the associated $L^1(0,1)\times\mathbb{R}_+$ product space with respect to the measurement uncertainty are derived in terms of the maximum interval between successive sampling instants. This condition also implies the exponential convergence of the observer in absence of measurement uncertainty. The result is validated using numerical simulations for a representative case study with non-monotonic Haldane growth rate and compared to the results of a continuous–discrete EKF for the approximated numerical model. These comparisons show that the proposed observer achieves a similar accuracy in its approximated implementation then the EKF with a considerably lower computational effort.

7.2 | Outlook and future research

Future studies will consider more complex classes of cell population balance models, the combination of discrete-time and continuous-time measurements including stochastic components and time-delays, as well as experimental implementation and validation of the observer.

ACKNOWLEDGMENT
The results presented in this article are part of a research project supported by the Deutsche Forschungsgemeinschaft (DFG, German Research Foundation)—Project-ID 395461267.

10991239, 2022, 2, Downloaded from https://onlinelibrary.wiley.com/doi/10.1002/mc.5852 by Karlsruher Institut Fur Technologie, Wiley Online Library on [19/11/2026]. See the Terms and Conditions (https://onlinelibrary.wiley.com/terms-and-conditions) on Wiley Online Library for rules of use; OA articles are governed by the applicable Creative Commons License

CONFLICT OF INTEREST

The authors declare that there is no conflict of interest for this article.

DATA AVAILABILITY STATEMENT

Data sharing is not applicable to this article as no new data were created or analyzed in this study.

ORCID

Alexander Schaum https://orcid.org/0000-0002-2710-1851

REFERENCES

1. Mhaskar P, Hjortso MA, Henson M. Cell population modeling and parameter estimation for continuous cultures of saccharomyces cerevisiae. *Biotechnol Prog*. 2002;18:1010-1026.
2. Daoutidis P, Henson M. Dynamics and control of cell populations in continuous bioreactors. Proceedings of the AIChe Symposium Series; Vol. 326, 2002:274-289.
3. Mantzaris NV, Daoutidis P. Cell population balance modeling and control in continuous bioreactors. *J Process Control*. 2004;14:775-784.
4. Vollmer U, Raisch J. Control of batch crystallization a system inversion approach. *Chem Eng Process Process Intensificat*. 2006;45(10):874-885. Particulate processes a special issue of chemical engineering and processing. doi:10.1016/j.cep.2006.01.012
5. Palis S, Kienle A. Discrepancy-based control of particulate processes. *J Proc Control*. 2014;24:33-46.
6. Rocha-Cozatl E, Moreno JA, Wouver AV. Application of a continuous-discrete unknown input observer to estimation in phytoplanktonic cultures. *IFAC Proc Vol*. 2012;45(15):579-584.
7. Krämer D, King R. On-line monitoring of substrates and biomass using near-infrared spectroscopy and model-based state estimation for enzyme production by S. Cerevisiae. Proceedings of the 2005 IEEE Computer Society Conference on Computer Vision and Pattern Recognition (CVPR'05); 2016:609-614.
8. Jerono P, Schaum A, Meurer T. Observer design for the droop model with biased measurement: application to Haematococcus pluvialis. Proceedings of the 57th IEEE CDC; 2018:6295-6300; Miami, FL.
9. Jerono P, Schaum A, Meurer T. Moment-based Kalman filter design for cell population balance models in batch fermentation processes. Proceedings of the IFAC AdChem 2021; 2021; Venice, Italy.
10. Goffaux G, Wouver AV, Bernard O. Continuous - discrete interval observers for monitoring microalgae cultures. *Biotechnol Progr*. 2009;25(3):667-675.
11. Mazenc F, Dinh TN. Continuous-discrete interval observers for systems with discrete measurements; 2013:787-792.
12. Mazenc F, Dinh TN. Construction of interval observers for continuous-time systems with discrete measurements. *Automatica*. 2014;50:2555-2560.
13. Hernandez H, Alvarez J. Robust estimation of continuous nonlinear plants with discrete measurements. *J Process Control*. 2003;13:69-89.
14. Jerono P, Schaum A, Meurer T. Observability analysis and robust observer design for a continuous yeast culture. *J Proc Control*. 2021;104:62-73.
15. Ji L, Rawlings JB. Application of MHE to large-scale nonlinear processes with delayed lab measurements. *Comput Chem Eng*. 2015;80:63-72.
16. Ji L, Rawlings JB, Hu W, Wynn A, Diehl M. Robust stability of moving horizon estimation under bounded disturbances. *IEEE Trans Automat Contr*. 2016;61(11):3509-3514.
17. Feketa P, Schaum A, Jerono P, Meurer T. Impulsive observer design for a class of continuous biological reactors. Proceedings of the 58th IEEE Conference on Decision and Control (CDC); 2019; Nice, France.
18. Sontag ED. Smooth stabilization implies coprime factorization. *IEEE Trans Automat Contr*. 1989;34(4):435-443.
19. Hespanha J, Liberzon D, Teel A. Lyapunov conditions for input-to-state stability of impulsive systems. *Automatica*. 2008;44(11):2735-2744.
20. Dashkovskiy S, Mironchenko A. Input-to-state stability of nonlinear impulsive systems. *SIAM J Control Optim*. 2013;51(3):1962-1987.
21. Feketa P, Bajcinca N. On robustness of impulsive stabilization. *Automatica*. 2019;104:48-56.
22. Hu W, Zhu Q, Karimi HR. Some improved Razumikhin stability criteria for impulsive stochastic delay differential systems. *IEEE Trans Automat Contr*. 2019;64(12):5207-5213.
23. Hu W, Zhu Q. Moment exponential stability of stochastic nonlinear delay systems with impulse effects at random times. *Int J Robust Nonlinear Control*. 2019;29(12):3809-3820.
24. Hu W, Zhu Q, Karimi HR. On the p-th moment integral input-to-state stability and input-to-state stability criteria for impulsive stochastic functional differential equations. *Int J Robust Nonlinear Control*. 2019;29(16):5609-5620.
25. Zhu Q. Stabilization of stochastic nonlinear delay systems with exogenous disturbances and the event-triggered feedback control. *IEEE Trans Automat Contr*. 2019;64(9):3764-3771.
26. Zhu Q. p-th moment exponential stability of impulsive stochastic functional differential equations with Markovian switching. *J Franklin Inst*. 2014;351(7):3965-3986.
27. Zhang M, Zhu Q. New criteria of input-to-state stability for nonlinear switched stochastic delayed systems with asynchronous switching. *Syst Control Lett*. 2019;129:43-50.
28. Karafyllis I, Krstic M. *Input-to-State Stability for PDEs*. Springer; 2018.

10991239, 2022, 2, Downloaded from https://onlinelibrary.wiley.com/doi/10.1002/mc.5852 by Karlsruher Institut Fur Technologie, Wiley Online Library on [19/11/2026]. See the Terms and Conditions (https://onlinelibrary.wiley.com/terms-and-conditions) on Wiley Online Library for rules of use; OA articles are governed by the applicable Creative Commons License

29. Schaum A, Jerono P, Meurer T, Moreno JA. Moment-based dissipative observer design for cell population balance models. Proceedings of the IFAC AdChem; 2021; Venice, Italy.
30. Christofides PD, El-Farra N, Li M, Mhaskar P. Model-based control of particulate processes. *Chem Eng Sci*. 2008;63(5):1156-1172. Control of Particulate Processes. doi:10.1016/j.ces.2007.07.017
31. Mesbah A, Huesman AEM, Kramer HJM, de Hof PMJV. A comparison of nonlinear observers for output feedback model-based control of seeded batch crystallization processes. *J Process Control*. 2011;21(4):652-666.
32. Fridman E, Blighovsky A. Robust sampled-data control of a class of semilinear parabolic systems. *Automatica*. 2012;48(5):826-836. doi:10.1016/j.automatica.2012.02.006
33. Villadsen J. On the use of population balances. *J Biotechnol*. 1999;71:251-253.
34. Jerono P, Schaum A, Meurer T. Parameter identification of a yeast batch cell population balance model. Proceedings of the IFAC SysId; 2021; Padova, Italy.
35. Atzori F, Jerono P, Schaum A, Baratti R, Tronci S, Meurer T. Identification of a cell population model for algae growth processes. Proceedings of the IFAC SysId; 2021; Padova, Italy.
36. Beniich N, Abouzaid B, Dochain D. On the existence and positivity of a mass structured cell population model. *Appl Math Sci*. 2018;12(19):921-934.
37. Sontag ED. On the input-to-state stability property. *Eur J Control*. 1995;1(1):24-36.
38. Dettman JW. *Mathematical Methods in Physics and Engineering*. Dover Publications, McGraw-Hill; 1988.
39. Dashkovskiy S, Feketa P. Asymptotic properties of Zeno solutions. *Nonlinear Anal Hybrid Syst*. 2018;30:256-265.
40. Khalil H. *Nonlinear Systems*. 2nd ed. Prentice-Hall; 1996.
41. Mancilla-Aguilar JL, Haimovich H, Feketa P. Uniform stability of nonlinear time-varying impulsive systems with eventually uniformly bounded impulse frequency. *Nonlinear Anal Hybrid Syst*. 2020;38:100933.
42. Aris R. *Introduction to the Analysis of Chemical Reactors*. Prentice-Hall; 1969.
43. Dochain D, Perrier M, Ydstie B. Asymptotic observers for stirred tank reactors. *Chem Eng Sci*. 1992;47(15/16):4167-4177.
44. Schaum A, Jerono P. Observability analysis and observer design for a class of cell population balance models. *IFAC-PapersOnLine*. 2019;52(2):189-194.
45. Gelb A. *Applied Optimal Estimation*. MIT Press; 1978.
46. Schaum A, Moreno JA, Vargas A. Global observability and detectability analysis for a class of nonlinear models of biological processes with bad inputs. Proceedings of the 2nd IEEE International Conference on Electrical and Electronics Engineering, (ICEEE) and XI Conference on Electrical Engineering (CIE); 2005:343-346.
47. Schaum A, Moreno JA. Dynamical analysis of global observability properties for a class of biological reactors. Proceedings of the 10th IFAC International Symposium on Computer Applications in Biotechnology (CAB); 2007: 209-214; Cancun, Mexico.
48. Gauthier JP, Hammouri H, Othman S. A simple observer for nonlinear systems: applications to bioreactors. *IEEE Trans Automat Contr*. 1992;37(6):875-880.
49. Schaum A, Alvarez J, Lopez T. Saturated PI control for continuous bioreactors with Haldane kinetics. *Chem Eng Sci*. 2012;68(1):520-529.
50. Badillo-Hernandez U, Alvarez-Icaza L, Alvarez J. Model design of a class of moving-bed tubular gasification reactors. *Chem Eng Sci*. 2013;101:674-685.
51. Franco-de los Reyes HA, Schaum A, Meurer T, Alvarez J. Stabilization of an unstable tubular reactor by nonlinear passive output feedback control. *J Process Control*. 2020;93:83-96.

How to cite this article: Schaum A, Jerono P, Feketa P. Robust impulsive observer design for infinite-dimensional cell population balance models. *Int J Robust Nonlinear Control*. 2022;32(2):774-791. doi: 10.1002/rnc.5852

10991239, 2022, 2, Downloaded from https://onlinelibrary.wiley.com/doi/10.1002/rnc.5852 by Karlsruher Institut Fur Technologie, Wiley Online Library on [19/11/2026]. See the Terms and Conditions (https://onlinelibrary.wiley.com/terms-and-conditions) on Wiley Online Library for rules of use; OA articles are governed by the applicable Creative Commons License